A.W. BYDAŁEK*,****#, W. WOŁCZYŃSKI**, A. BYDAŁEK***, P. SCHLAFKA****, P. KWAPISIŃSKI*****

ANALYSIS OF SEPARATION MECHANISM OF THE METALLIC PHASE OF SLAG IN THE DIRECT-TO-BLISTER PROCESS

ANALIZA MECHANIZMU WYDZIELANIA FAZY METALICZNEJ W ŻUŻLU ZAWIESINOWYM

The article discusses the structure of the slag in the liquid state, the properties and interactions within the slag. The analysis of structures occurring in slag suspension were presented with regard to differences in chemical composition in micro-areas. Two different mechanisms for formation of precipitates in Cu-Fe-Pb alloys during extraction were showed.

Keywords: decopperised, crystallisation, slag, structure.

W artykule omówiono strukturę żużli w stanie ciekłym, oraz właściwości i oddziaływania wewnątrz żużli. Przedstawiono wyniki analiz występujących struktur w żużlu zawiesinowym, w odniesieniu do różnic w składzie chemicznym w mikroobszarach. Wskazano na dwa różne mechanizmy tworzenia wydzieleń stopu Cu-Fe-Pb podczas ekstrakcji.

1. Analysis of the problems

1.1. Introduction

Increasing metallurgical yields and improving quality of the metals/alloys requires introducing numerous processes and techniques during designing of solidification, melting and casting. These are, reported in literature, reducing metals oxides present within slags [1-3], melt protecting with fluxes [4], melt modification before casting into foundry molds [5,6], riser protecting with insulating sleeves against surplus heat loses [7] as well as considering back-diffusion phenomena in solidifying metals and alloys [8]. The present paper deals with suspension slags of Cu production, their structure, composition, and mechanisms of extraction processes which proceed inside the slags.

Suspension slag is formed during the extraction process of copper production in the melting flash. Then-formed suspension slag is directed to the electric furnace-arc where it is decopperisied. Decopperisation causes the reduction of oxides forms of primarily copper, lead and iron and then segregation of a Cu-Fe-Pb alloy. The moment of slag contacting the layer of coke reduction (phase 1), the majority of Cu_2O is removed and the total copper content of the slag decreases to approx. 2,0%.

Over the next 4-5 hours (phase 2) of the process, the content decreases to approx. 0.8%. Following the tapping process (phase 3), the content keeps decreasing and reaches a minimum of approx. 0.5%. The changes of concentration in the slag (particularly in phase 2 and 3) affect the structure and properties what have the decisive impact on the slag suspension decopperisation.

1.2. The structure of slag in the liquid state

The properties of the slag are determined by its structure. Slag structure can be described either by the molecular theory [1] or can be analyzed as electrolytes [2]. A.Bydałek and M. Brzózka [3] assumed that the slags in the liquid state were the boundary type of strong electrolyte solutions. In that case slag has ordered construction of the ion and tend to surround cations with oxygen ions. Small ions with high charge (Si^{4+}, B^{3+}) strongly attract oxygen and produce a significant density of their immediate environment. Large ions with low charges (Ca^{2+}, Na^{1+}) weakly attract oxygen.

Tiemkina [9,14] however, pointed that, the creation of a multi-component systems of ionic complexes- rather than the individual components of the ion- is still a major obstacle in the

*   AGH UNIVERSITY OF SCIENCE AND TECHNOLOGY, FACULTY OF NON-FERROUS METALS, AL. A. MICKIEWICZA 30, 30-059 KRAKÓW, POLAND
**   INSTITUTE OF METALLURGY AND MATERIALS SCIENCE OF POLISH ACADEMY OF SCIENCES, 25 REYMONTA STR., 30-059 KRAKOW, POLAND
***   STATE HIGHER VOCATIONAL SCHOOL IN GŁOGÓW, GŁOGÓW, POLAND
****   UNIVERSITY OF ZIELONA GÓRA, FACULTY OF MECHANICAL ENGINEERING, ZIELONA GÓRA, POLAND
***** METALLURGY DEPARTMENT, KGHM POLSKA MIEDŹ S.A., LUBIN, POLAND

\#   Corrersponding author: abydalek@agh.edu.pl

analysis of local ordered conditions. Other studies [11-13] show occurrence of additional melted (melting) and breaking of silicate tetrahedral bridges. Such a phenomenon is enhanced particularly in the presence of compounds such as CaO, Na_2O and K_2O.

An important factor contributing to the formation of metallic phases of solid slag may be also a segregation of the ingredients during solidification process (including during eutectic solidification [14-17]). The existence of concentration gradient causes the diffusion in the solid state during the crystallization. At the same time, the diffusion phenomenon enhances elimination of segregation [17]. Segregation and diffusion affect mostly the changes of physico-chemical properties during the processes of slag-cleaning.

Considering the mentioned above aspects this article aims at the analysis of structures existing in the slag of direct-to-blister process, considering the differences in the chemical composition in micro-areas.

1.3. Properties and interactions

The impact of active ingredients of melting atmosphere on the processes occurring during the slag extraction, is a continuous disruption of thermodynamic equilibrium between the slag (S), extracted metal-containing compound (WN), metal (M) and atmosphere (A) [15,18-22]. Physico-chemical properties of slag are depended on its structure. Meanwhile mass transfer processes are related to the properties of the entire system A-S-WN-M.

Simplifying the approach [2,23], the kinetics of extraction of slag and metal compounds, depends on the viscosity of slag. The composition of gases in the atmosphere [18] and interaction with the extracted metal phase [25], as well as temperature [24], are main factors affecting viscosity. The complexes of e.g. MgO and SiO_2 increase the viscosity [23,26] as well as surface tension [24], and are characterized by a high chemical affinity to Cu_2O [23-25]. Meanwhile, other studies [26] have shown that there is no direct/clear correlation between viscosity and surface tension. In simple systems, an increased ratio of CaO / SiO shows first decrease and then increase of viscosity, with surface tension steadily increasing. The impact of extracted metal in the slag phase might be described by the theory of so-called electrical double layer [1]. The difference in potentials detected at the interface, is described by Coulomb Dietl [27] and is associated with remoteness from equilibrium conditions. Decisive role was also attributed to mixing of slag and metal precipitates [28]. However, in that case, assuming the blending of slag with the extracted metal alloy excludes the Nernst approach. The temporal variability of S-M interactions can be also analyzed by means of Planck's formula [10], which describes the work function of molecules transferring from one phase to another.

Analysis of separation mechanism of the metallic phase in the slag suspension is presented to identify the drivers of changes in the properties of the slag due to the suspension formed in the structure.

2. Analysis of the structure of slag

The composition of slag suspension is presented in Table 1. Samples were collected during charge of slag into electric furnace. Then collected material was melted in an electric furnace under reducing conditions and cast into a metal mold.

TABLE 1

The basic chemical composition of the flash furnace slag used for analysis

	Cu	Ag	Pb	Fe	S	As
Slag, % mass	13,64	0,014	3,2	6,24	0,042	0,180

The structure shown in Figure 1 is a coat layer between the two test areas, distinguished during the research: area of coagulation of spherical precipitates – mainly Cu-Fe-Pb (area I) and the isolation and crystallization area of metal phase – mainly Cu-Fe-Pb (area II). The following figures show further distinguished areas. Figs 2 and 3 show the structures of area I, highlighting the region Ia – with no fermata-shape phases (Fig. 2), and the area Ib – with presence of fermata-shape phases (Fig. 3). Fig. 4 shows results from the structure analyses of area II.
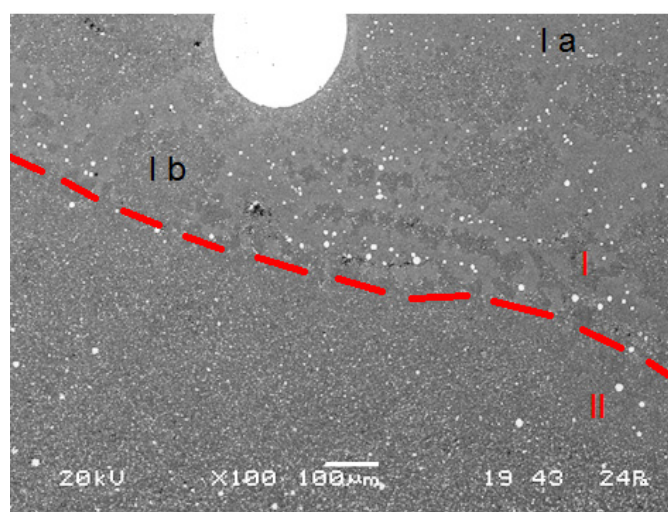

Fig. 1. The image of coat layer: I – coagulation area with spherical precipitates of Cu-Fe-Pb slag; Ia – no fermata-shape phase, and Ib – with the presence of fermata-shape phase; II – precipitates zone and crystallization of a Cu-Fe-Pb from the slag suspension

Figure 2 shows the structure of the dispersion of fine precipitates rich in silicon, iron, calcium, copper, and large metal separations containing copper, iron and lead – Cu-Fe-Pb alloy. Such structures characterizes with two types of precipitates of Cu-Fe-Pb. First type shows large – 100-150 microns – precipitates separation. Second type – a small flocculent precipitates of Cu-Fe-Pb alloy – is of the size of approx. 5 microns.

The analysis of the chemical composition of areas surrounding these two types of precipitates (Fig. 2) showed differences in composition occurring in immediate environment precipitates. The first type of precipitates showed the following content:

a)

b)

1 - the area with finely disperse precipitates of - silicon, iron, calcium, copper, aluminum, lead, magnesium, potassium, zinc, oxygen

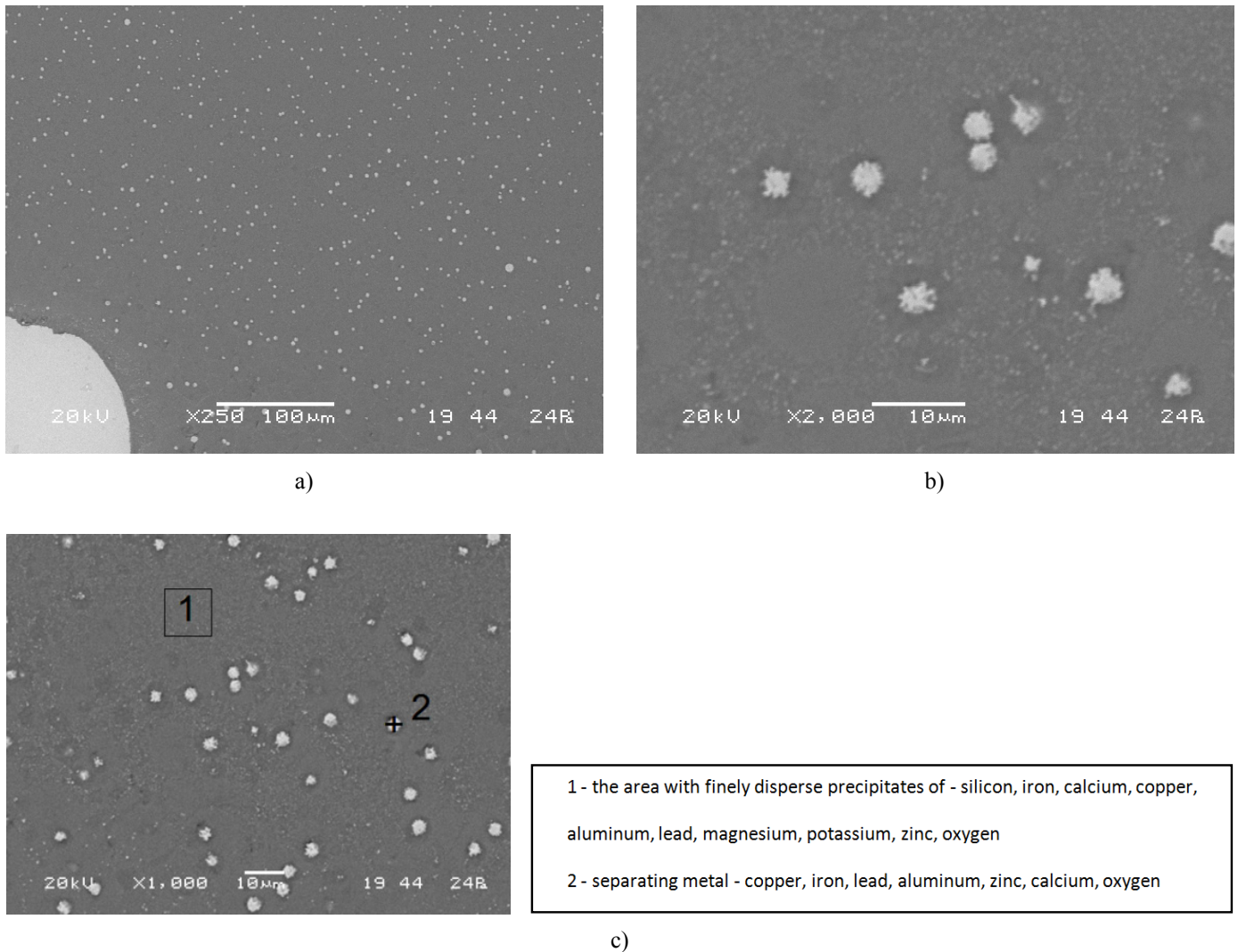2 - separating metal - copper, iron, lead, aluminum, zinc, calcium, oxygen

c)

Fig. 2. The structures of Ia area with the spherical precipitates of Cu-Fe-Pb (according to Fig. 1 – no fermata-shape phase into the slag suspension): a) slag suspension with separation of the first type, b) second type of slag suspension with precipitates, c) the marked areas of analysis and the summary of chemical microanalysis

Si – 20.2% Ca – 15.2% Fe – 10.7% Cu – 6.9%, Pb – 3.4%, K – 1.1%. Meanwhile, the surroundings of precipitates of second type were characterized with: Si – 21.1%, Pb – 13.1% Cu – 9.8%, Ca – 7.8%, Fe – 6.6%, F – 5.5%.

The structure of the area defined as Ib presented on Fig. 3, contains mainly crystalline fermata-shape structure (area 1 in Fig. 3c) with precipitates of the second type distributed at grain boundaries of Cu-Fe-Pb alloy. On the contrary, crystalline precipitates of first type (separation 3 in Fig. 3c) are distributed outside the structures of the Cu-Fe-Pb alloy. Chemical microanalysis of composition revealed the presence of dendritic fermata-shape (Si – 18%, Fe – 15.7% Ca – 10.9% Cu – 6.3%, Pb – 4.9%, K – 1, 9%) in crystal structures. The same analysis showed slag matrix being composed of Si – 17.2% Fe – 13.3% Cu – 10.9%, Ca – 10.6%, Pb – 5.9%, K – 2.7%.

The separations (as in Fig. 3a) indicating the dissolution of previously formed separating Cu-Fe-Pb alloy of the first type by the expansion of dendritic structure were found particularly interesting. Indirect evidence on such a mechanism could be mi-croanalysis of separation that indicates lower copper content (Cu – 22%, more iron Fe – 11.4%, and lead Pb – 5.9%) in comparison with other precipitates (mean: Cu – 69% Fe – 4.5%, Pb – 3.5%).

Figure 4 shows structures of the II area – the area of separation and crystallization of a Cu-Fe-Pb alloy from slag suspension (Fig. 1). Microanalysis of the chemical composition of the whole area indicates the following content: Si – 18.3% Fe – 12.7% Ca – 10.6% Cu – 8.6%, Pb – 7.1% K – 2.8 %. Based on Fig. 4 the following sub-areas were identified within the II area:

– rods-type separating (1); silicon 18.3%, iron 12.7%, calcium 10.5%, copper 8.6, 7.1 lead, aluminum 5.9%, magnesium 3.0%, potassium 2.8%, zinc 1.6 %

– intestines-type separating (2); 36% iron, 8.7% silicon, 7.1% copper, 4.8% aluminum, 4.4% calcium, 3.3% magnesium, potassium 1.2%, lead 2.5%, zinc 2.6 %

– dark-gray "polygons" (3); silicon 20.3%, calcium 15.2%, 10.7% iron, 6.9% copper, 6.1% aluminum, 4.5% magnesium, lead 3.4%, potassium 1.2%,

a)

b)

1 - separation of dispersion in the structure of fermata,

2 - the area of the slag matrix without dispersion of precipitates,

3 - the area of slag from the dispersion matrix precipitates,

4 - fermata structure without precipitates

5 - separation of the first type of spherical fermata structure,

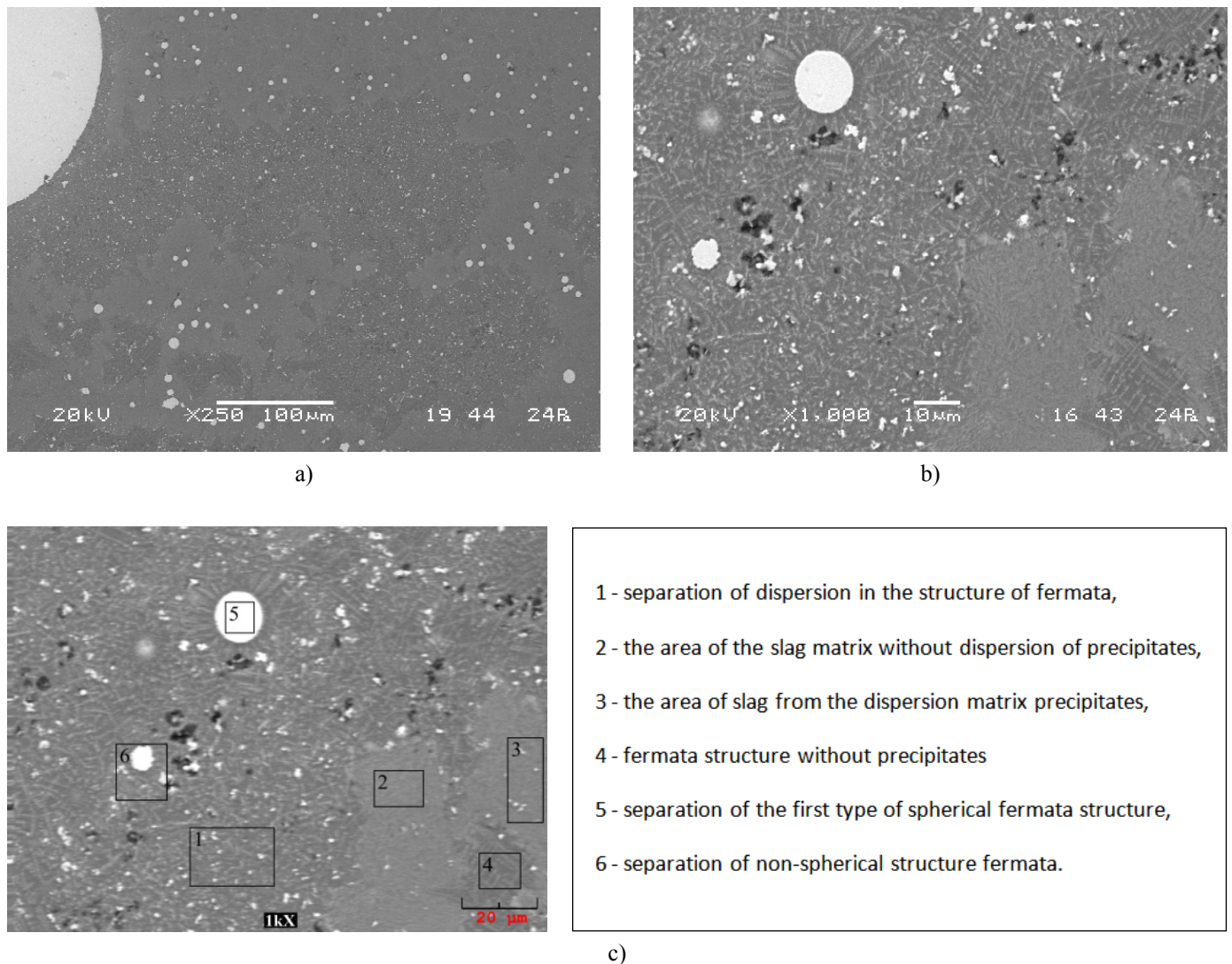6 - separation of non-spherical structure fermata.

c)

Fig. 3. Structure Ib of area with the crystalline precipitates according to Fig. 1 (presence of a suspension slag with the fermata-shape phase): a) slag suspension with large and small precipitates of the first and second type, b) the crystal fermata-shape structure of fine separation of the first type, with precipitates of second type being trapped in the spaces between grains, c) the marked areas of analysis and the summary of chemical microanalysis

–   gray filling areas (4); 20.12% silicon, lead 13.1%, copper 9.8%, 7.9% calcium, 6.6% aluminum, 6.6% iron, 5.4% potassium, 1.1% magnesium, zinc 1 7%.

Separation of metallic Cu-Fe-Pb (5), both of the first and second type are visible as well- however the shape is clearly not spherical.

3. Summary

The analysis of suspension slag structures shows that there are two mechanisms formatting the metallic phases of Cu-Fe-Pb:
–   direct separation and coagulation from the liquid slag (the region I in Fig. 1),
–   separation by the presence of crystallizing slag matrix (area II in Fig. 1).

In the first case, copper rich separating is obtained (approx. 70%), whereas in the second case separating is enriched – at the expense of copper content (copper approx. 50%) – by iron and lead. There are two types of precipitates to be distinguished: the large ones – bigger than 100 microns (designated as a type number one), and a few micrometers big, fine-dispersion ones (designated as a type number two). The analysis of the areas of short- and long-distance neighborhood of given precipitates were very interesting. They showed virtually homogenous composition around the precipitates formed directly from the liquid (Fig. 5a) and a variable composition in function of the distance as well as for the distribution, in the case of precipitates formed during crystallization of the slag fermata-shape phase (Fig. 5b and Fig. 6)

It is interesting that the share of such components as silicon, sodium, potassium and magnesium in those areas is very

a)

b)

1 - "rods" - silicon, calcium, aluminum, potassium, iron, lead, copper, oxygen

2 - gray "intestine" - iron, silicon, calcium, aluminum, magnesium, potassium, copper, lead, oxygen

3 - dark gray "polygons" - silicon, calcium, aluminum, magnesium, iron, copper, lead, oxygen

4 - gray areas filler - silicon, calcium, aluminum, potassium, lead, iron, copper, oxygen

5 - separation of metal - copper, iron, lead, calcium, aluminum, zinc, potassium, magnesium, oxygen
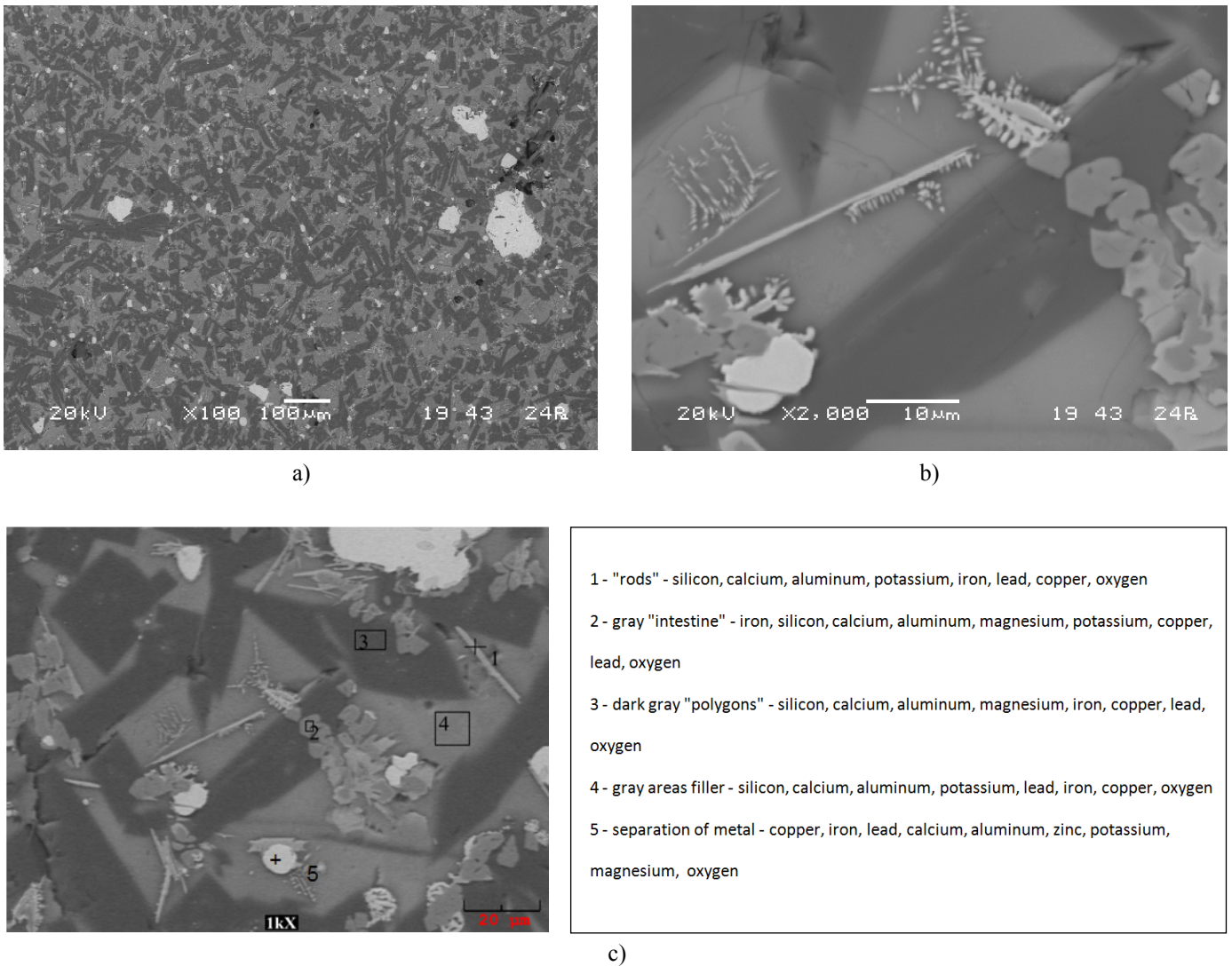
c)

Fig. 4. Structures of II area with the crystalline precipitates in the slag suspension: a) slag suspension with large and small precipitates of the first and second type, b) the crystal structure of fermata-shape with fine separations of the first and second type c) the marked areas of analysis and the summary of chemical microanalysis

variable. It could give a base for broader analysis of suspension slag in reference to already mentioned tendency to encircling oxygen cations by such ions as Si^{4+}, Ca^{2+}, Na^{1+}, particularly in terms of characteristics of oxide reduction process in suspension slag. It might also justify an argument for necessity of creating highly reducing conditions during the decopperised process of suspension slag.

The analysis described above concludes with the thesis for further research: both coagulation and coalescence phenomena, as well as crystallization fermata-shape phases are responsible for the secretion of metallic phase in slag suspension. Thus, it should be possible to take into account the descriptions concerning heterogeneity of concentration that occurs during the process of dendritic crystallization of such multiphase system as slag suspension. It must be assumed that the segregation of components determines the properties of the Cu-Pb-Fe alloy that excretes in the slag slurry. Being in favor of fermata-shape phases, the processes of dissolution of Cu-Fe-Pb precipitates may also be the main causes of changes of viscosity of suspension slag.

REFERENCES

[1] H. Schenck, Die Physikalische Chemie der Eisenhűttenprozesse, T. III, Berlin, (1934).

[2] A. Staronka, Hutnik **23**, 3, 110-118 (1956).

[3] M. Brzózka, A. Bydałek: Archiwum Technologii Budowy Maszyn, 5, 7-12 (1984).

Spherical precipitates of the first kind

Basic elements	Medium composition,%
Cu	70
Fe	4,5
Pb	3,5

a)

Surrounding of precipitates

Basic elements	Medium composition,%
Si	20
Ca	15
Fe	10
Cu	7
Al	6
Mg	4
Pb	3,5
K	1

"Flocculent" precipitates of the second type

b)

Basic elements	Medium composition,%
Cu	20
Fe	12
Pb	6

Surrounding of precipitates

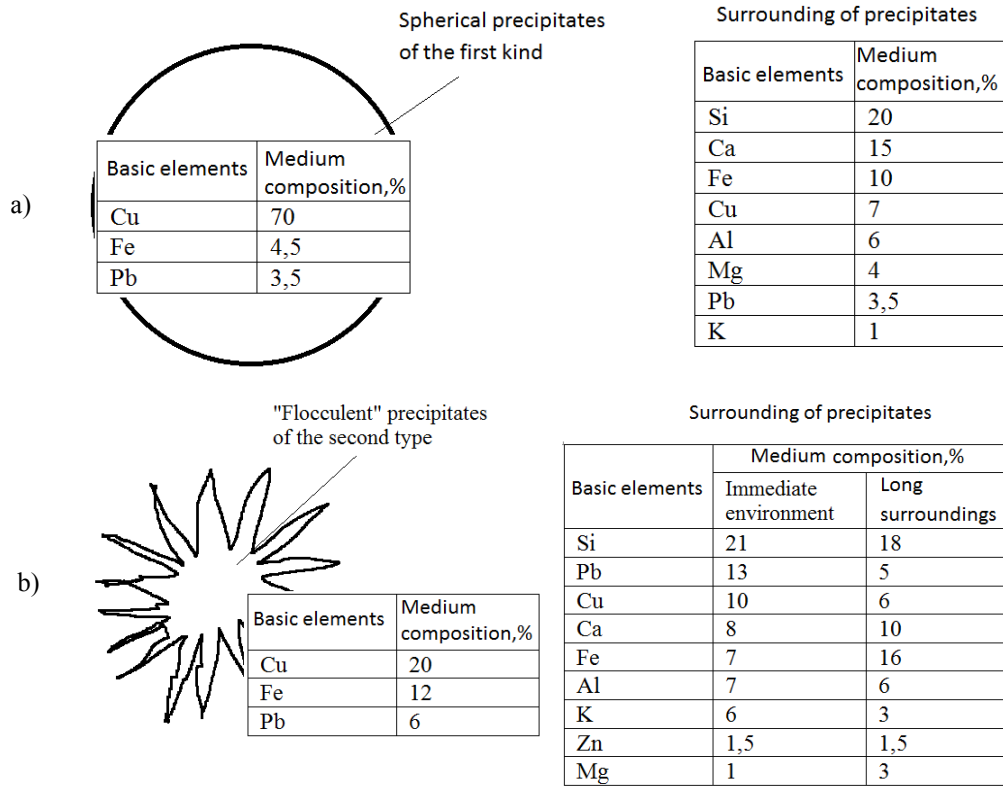| Basic elements	Medium composition,%	
	Immediate environment	Long surroundings
Si	21	18
Pb	13	5
Cu	10	6
Ca	8	10
Fe	7	16
Al	7	6
K	6	3
Zn	1,5	1,5
Mg	1	3

Fig. 5. The image of transfer layer: a) spherical separation of Cu-Fe-Pb alloy from the coagulation of slag (Ia – no fermata-shape phase – Fig. 1), b) "flocculent" separation of Cu-Fe-Pb alloy from the coagulation of slag with participation of crystalline phases (Ib – presence of fermata-shape phase)

Separated from the II area

Basic elements	Medium composition,%	
	Precipitates of the ferst kind	Precipitates of the second kind
Cu	50	12
Fe	10	18
Pb	4	6

Surrounding of precipitates

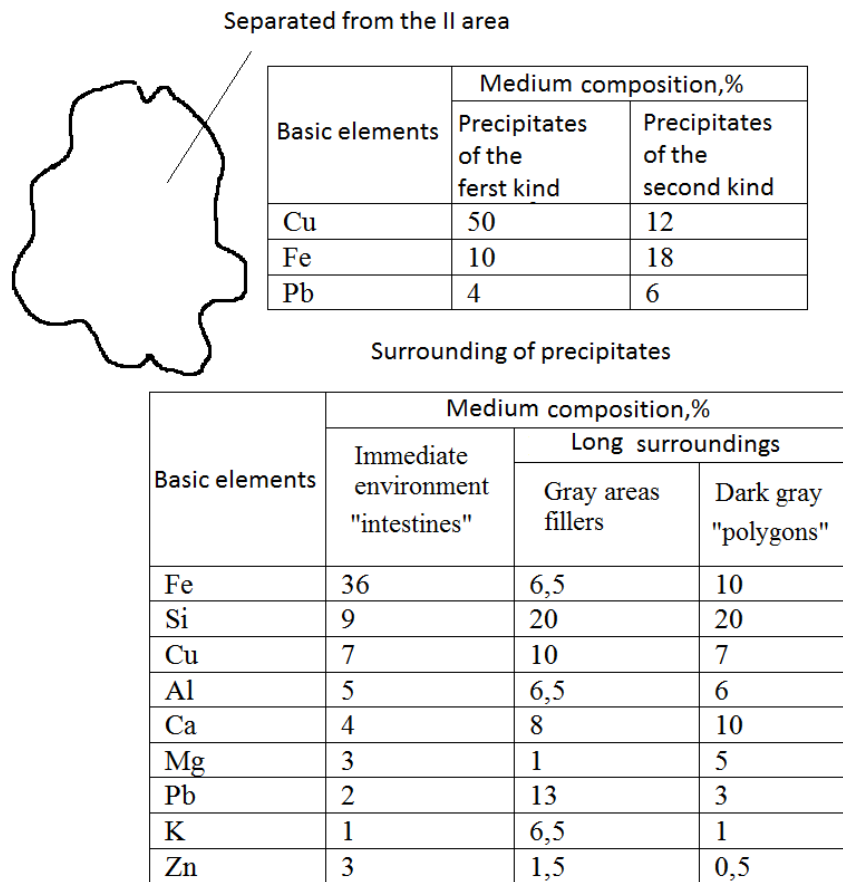| Basic elements	Medium composition,%		
	Immediate environment "intestines"	Long surroundings	
		Gray areas fillers	Dark gray "polygons"
Fe	36	6,5	10
Si	9	20	20
Cu	7	10	7
Al	5	6,5	6
Ca	4	8	10
Mg	3	1	5
Pb	2	13	3
K	1	6,5	1
Zn	3	1,5	0,5

Fig. 6. The image of transfer layer with non-spherical separation of Cu-Fe-Pb alloy from the second area of isolation and crystallization of suspension slag (with presence of the fermata-shape phase)

[4]   W.K. Krajewski, G. Piwowarski, P.K. Krajewski, Protecting melted zinc-aluminium based foundry alloys against hydrogen pick-up, Archives of Metallurgy and Materials **59**, 2, 501-503 (2014).

[5]   W. Krajewski, The effect of Ti addition on properties of selected Zn-Al alloys, Physica Status Solidi A-Applied Research **147**, 389-399 (1995).

[6]   W.K. Krajewski, A.L. Greer, P.K. Krajewski, Trends in developments of high-aluminium zinc alloys of stable structure and properties, Archives of Metallurgy and Materials **58**, 859-861 (2013).

[7]   W.K. Krajewski, J.S. Suchy, Determining thermal properties of insulating sleeves, Solidification and GravityVBook Series: Materials Science Forum **649**, 487-491 (2010).

[8]   W. Wolczynski, W. Krajewski, R. Ebner, J. Kloch, The use of equilibrium phase diagram for the calculation of non-equilibrium precipitates in dendritic solidification. Theory, Calphad-Computer Coupling of Phase Diagrams and Thermochemistry **25**, 3, 401-408 (2001).

[9]   E. Becker, Wartmetall Reduktion aus NE -Metall Schlackenschmelzen, Studienarbeit Inst. Metallkunde und Elektrometallurgie, RWT Achen (1987).

[10]   A. Yazawa, Y. Tokeda, Metallurgical Review of MMIJ **4**, 1, 53-57 (1987).

[11]   P. Migas**,** M. Karbowniczek, Archives of Metallurgy and Materials **55**, 4, 1147-1157 (2010).

[12]   A.W. Bydałek, A. Bydałek, W. Wołczyński, S. Biernat, Archives of Metallurgy and Materials **60**, 1, 323-326 (2015).

[13]   J. Bockris, J.W. Tomilson, J.L. White, Journal of the Chemical Society, Faraday Transactions **52**, 663-671 (1956).

[14]   A.W. Bydałek, W. Wołczyński, A. Dytkowicz, Krzepnięcie Metali i Stopów **37**, 26-29 (1998).

[15]   T. Himemiya, W. Wołczyński, Materials Transactions of the Japan Institute of Metals **43,** 2890-2896 (2002).

[16]   W. Wołczyński, E. Guzik, W. Wajda, D. Jędrzejczyk, B. Kania, M. Kostrzewa, Archives of Metallurgy and Materials **57**, 105-117 (2012).

[17]   W. Wołczyński, Mathematical Modeling of the Microstructure of Large Steel Ingots, Entry in: The Encyclopedia of Iron, Steel, and Their Alloys, Eds. Taylor & Francis Group, New York-USA, 2015 (*in print*).

[18]   A. Bydałek, Prace Naukowe Politechniki Wrocławskiej, Instytut Chemii Nieorganicznej i Metalurgii, 17, 183-186 (1973).

[19]   S. Simonow, T. Sakai, M, Maeda, Metallurgical Transactions, B23B, 323-326 (June 1992).

[20]   A.W. Bydałek, A. Bydałek, Archives of Foundry Engineering **14**, 1, 21-24 (2014).

[21]   S. Biernat, A. W. Bydałek, Archives of Foundry Engineering **14**, 3, 85-89 (2014).

[22]   A.W. Bydałek, S. Biernat, A. Bydałek, P. Schlafka, International Journal of Engineering and Innovative Technology (IJEIT) **4**, 5, 186-193 (Nov. 2014).

[23]   M. Kucharski, T. Sak, P. Madej, M. Wędrychowicz, Metallurgical and Materials Transactions B – Process Metallurgy and Materials Processing Science **45B**, 2, 590-602 (2014).

[24]   J. Kowalczyk, M. Mroz, A. Warczok, T.A. Utigard, Metallurgical and Materials Transactions **B26B**, 1217-1223 (Dec. 1995).

[25]   A. Gierek, T. Karwan, J. Rojek, J. Szymek, Rudy i Metale, R.**50**, 12, 669-675 (2005).

[26]   A. Łedzki, P. Migas, R. Stachura, A. Klimczyk, M. Bernasowski, Archives of Metallurgy and Materials **54**, 2, 499-509 (2009).

[27]   M. Berwis, A. Schelbat, Giesserei, 2, 53-57 (1979).

[28]   A. Łedzki, P. Migas, R. Stachura, A. Klimczyk, M. Bernasowski, Archives of Metallurgy and Materials **54**, 1, 129-135 (2009).